

Effect of magnetic order on the fluorescence dynamics of TbF_3

M. F. Joubert and B. Jacquier

Laboratoire de Physico-Chimie des Matériaux Luminescents, Université Lyon I, 69622 Villeurbanne, France

R. L. Cone

Physics Department, Montana State University, Bozeman, Montana 59717

(Received 23 October 1986; revised manuscript received 2 February 1987)

The dynamical properties of Tb^{3+} fluorescence in TbF_3 have been investigated above and below its ferromagnetic phase transition ($T_C = 3.95$ K). Near and below T_C the magnetic interactions lead to splittings and shifts of the optical lines reflecting the interionic interactions and the onset of the ordered state. A dramatic (factor of 10) lengthening of the exciton decay occurs both when lowering the temperature below T_C and when applying an appropriate external magnetic field along the easy axis above T_C . Throughout the range from 300 to 1.6 K, the experimental fluorescence decays are in agreement with a rate-equation model involving fast-diffusion energy transfer among intrinsic ions. The observed decrease in diffusion coefficient can be understood either as the result of a large reduction of the resonant energy transfer between intrinsic ions or as the result of a decrease in the trapping probability in the ferromagnetic or aligned paramagnetic phases. Either process may be understood in terms of the short-range Tb^{3+} - Tb^{3+} interactions and the properties of the ordered state.

I. INTRODUCTION

Trivalent rare-earth ions in single-crystal hosts generate intense fluorescence from the ultraviolet to the infrared spectral region. This has given rise to numerous applications such as phosphors, fluorescent screens, and solid-state lasers. Optimization of fluorescence quantum efficiency and other properties requires the study of various parameters such as temperature, concentration, and excitation density. It is, for example, well known that an increase in rare-earth concentration generally leads to a reduction of the fluorescence quantum yield; however, this so-called concentration quenching is not always understood. It is accepted that this effect is due to rare-earth-ion-rare-earth-ion interactions which cannot be neglected in concentrated materials. Those interactions allow excitation energy transfer between the active ions, and therefore they are responsible for deexcitation by pathways other than radiative emission by the originally excited rare-earth centers.

When the rare-earth concentration reaches 100%, a complete delocalization of the excitation energy may exist, involving energy migration between quiresonant active ions. This excitonic behavior has been demonstrated recently in $\text{Gd}(\text{OH})_3$,^{1,2} GdCl_3 ,^{1,2} PrAlO_3 ,³ $\text{Tb}(\text{OH})_3$,⁴ and TbVO_4 .⁵ The elucidation of the nature of the dominant interaction—electric multipole interaction, electronic exchange or superexchange, magnetic dipole-dipole coupling, or virtual phonon exchange—is one of the main purposes for studies of energy migration.

With that goal, we have recently analyzed the dynamical properties of terbium fluorescence in several concentrated materials in which the cation environments are different:⁶ TbF_3 , TbAlO_3 , TbPO_4 , and $\text{Tb}(\text{C}_2\text{H}_5\text{SO}_4)_3 \cdot 9\text{H}_2\text{O}$. That body of work suggests a short-range interaction to be the dominant energy-transfer

coupling mechanism between intrinsic Tb^{3+} ions. This has been determined from the evolution of the resonant energy-transfer process when the temperature falls to the magnetic transition point and below.⁷ Among the interactions mentioned above, the electronic exchange or superexchange interaction is particularly characterized as a “short-range” coupling mechanism. Since the overlap of the electrons on two neighboring rare-earth ions is small, it is generally believed that a multicenter process involving the intervening ligands is equally or more important. That process is referred to as superexchange. Short-range interactions of this type are also well known from studies of the ground-state magnetic properties of concentrated compounds. The dynamical behavior of Tb^{3+} fluorescence spectra in concentrated materials near the critical temperature T_N or T_C has been described by others for the case of TbAlO_3 (Ref. 8) and $\text{Tb}_3\text{Al}_5\text{O}_{12}$.⁹

In this paper, we report the results of an investigation of the fluorescence dynamics of TbF_3 both above and below its ferromagnetic phase transition ($T_C = 3.95$ K). In Sec. II, we describe the material and the experimental setup. After a brief summary of the primary results on the fluorescence properties of TbF_3 in its paramagnetic phase at 4.4 K, the remainder of Sec. III is devoted to a presentation of the experimental data obtained in the ordered ferromagnetic state at 1.6 K and in the aligned paramagnetic state at 4.4 K with an external magnetic field applied along the easy magnetization axis. Finally, a discussion is presented regarding the validity of a fast-diffusion model for the optical excitation energy transfer when the material is both ferromagnetically ordered and disordered. In Sec. IV, two possible explanations are given for the dramatic increase in the intrinsic “incoherent exciton” lifetime in the ordered phases. One involves a reduction of quiresonant energy transfer between intrinsic ions when the homogeneous width be-

comes narrower than the inhomogeneous width—a “freezing out” of the energy-transfer process or “quasi-localization.” The second involves a reduction in the efficiency of trapping. A brief summary of the relationship of these TbF_3 results to those for other Tb^{3+} compounds is given in Sec. V.

II. TbF_3 MATERIAL AND EXPERIMENTAL DETAILS

The TbF_3 single crystals were grown at Hughes Laboratory by a Czochralski technique and were of excellent optical quality. The crystal symmetry is orthorhombic with four Tb^{3+} ions per unit cell; the space group is D_{2h}^{16} (P_{nma}), with rare-earth ions in a C_s environment.¹⁰ While the $(2J+1)$ -fold degeneracy of the free-ion states could be totally removed, the Stark-component scheme of the 5D_4 and 7F_6 multiplets of Tb^{3+} in TbF_3 , deduced from absorption and emission spectra at 25 K, shows the presence of several “quasidoublet” states.¹¹ In particular, the two lowest states in the 7F_6 ground multiplet are close together and are well separated from the next excited state which is around 115 cm^{-1} . At low temperature and zero magnetic field, the Tb^{3+} ion is a two-level singlet system which shows only induced magnetism; however, the paramagnetic singlet-singlet splitting is very small. In the ordered phase TbF_3 can be treated to an excellent approximation as a spin- $\frac{1}{2}$ Ising magnet with the characteristic near perfect anisotropy of the g value. The saturation moment is only slightly below the theoretical value for an $M_J = \pm 6$ doublet¹² ($8.95\mu_B$ versus $9\mu_B$).

In the ferromagnetic phase ($T_C = 3.95\text{ K}$) the local anisotropy constrains the Tb^{3+} moments to one of two axes in the (a, c) plane directed at $\pm 26^\circ$ with respect to the a axis.¹² This leads to a canted two-sublattice model for Tb^{3+} moments with a resultant ferromagnetic moment along the a axis. The first sublattice contains the two cations of the unit cell with coordinates $\pm(x, \frac{1}{4}, z)$ and the second one contains the two other cations of the unit cell with coordinates $\pm(x + \frac{1}{2}, \frac{1}{4}, \frac{1}{2} - z)$. Recently, neutron diffraction measurements have shown a small antiferromagnetic component of the magnetic moment in the b direction.¹³ Magnetization studies¹² at high fields applied along the c axis gave convincing evidence for a spin flip on one of the magnetic sublattices for $H_c = 13.1\text{ kOe}$ at 1.1 K. At higher temperatures it is reasonable to expect much higher fields to be required to realign the spins in that way.

At various temperatures between 1.6 and 300 K, the absorption, emission, and excitation spectra, as well as the fluorescence decays, were recorded with the use of conventional techniques described earlier.¹¹ A thin plate of TbF_3 of $1.53 \times 1.36 \times 0.625\text{ mm}^3$, oriented with a and b parallel to the shortest and longest dimensions respectively, was especially useful for polarization measurements and for spectroscopy in an external magnetic field. In the latter case, we used a liquid-helium superconducting magnet equipped to provide magnetic fields up to 40 kOe. As a result of the absence of a temperature-regulating device in this system, data were obtained only at pumped-helium temperature (1.6 K) or in the ambient-pressure liquid-helium bath (4.4 K).

III. EXPERIMENTAL RESULTS

A. Fluorescence properties above T_C

Before describing the new and significantly different experimental results obtained in the magnetically ordered phases of TbF_3 , we make a brief summary of the fluorescence properties of this material recorded at 4.4 K.¹¹ The absorption spectrum for the ${}^7F_6 \rightarrow {}^5D_4$ transitions of the Tb^{3+} ions is composed of six main lines as shown in Fig. 1(a). Their energies and their linewidths are indicated in Table I. The 5D_4 splittings at 4.4 K duplicate the ones observed at 25 K (Ref. 11) or at 77 K.¹⁴ After excitation in one of the 5D_4 Stark components, the blue emission (${}^5D_4 \rightarrow {}^7F_6$), presented in Fig. 2(a), results mainly from the deexcitation of Tb^{3+} ions perturbed by impurities or defects in the sample. The lowest 5D_4 Stark levels of these trap ions are populated by energy transfer from the far more numerous Tb^{3+} centers labeled “intrinsic” ions which are responsible for the absorption. The fluorescence located at about $20\,600\text{ cm}^{-1}$ emitted by the intrinsic ions decreases as the sum of two exponential functions, a fast one ($\tau = 179\ \mu\text{sec}$) characterizing the “incoherent-exciton” decay and a slow one ($\tau = 4\text{ msec}$) which is interpreted as the result of backtransfer from shallow traps. The decay of the deep-trap fluorescence at $20\,560\text{ cm}^{-1}$ exhibits an initial rise corresponding to the exciton decay and then decreases exponentially with a time constant of 5.4 msec. The excitation spectra of these two kinds of fluorescence are indistinguishable and correlate well with the intrinsic 5D_4 energy states derived from the absorption spectrum [Fig. 1(a)]. The proposed model, involving fast diffusion with trapping at shallow ($\Delta_1 \approx 10\text{ cm}^{-1}$) and deeper ($\Delta_0 \approx 40\text{ cm}^{-1}$) traps yields an effective diffusion coefficient of $8.6 \times 10^{-10}\text{ cm}^2/\text{sec}$ at 4.4 K.¹¹

Further indication of rare-earth–rare-earth interaction is provided by the existence of an exciton-exciton annihilation process. This mechanism is responsible for a

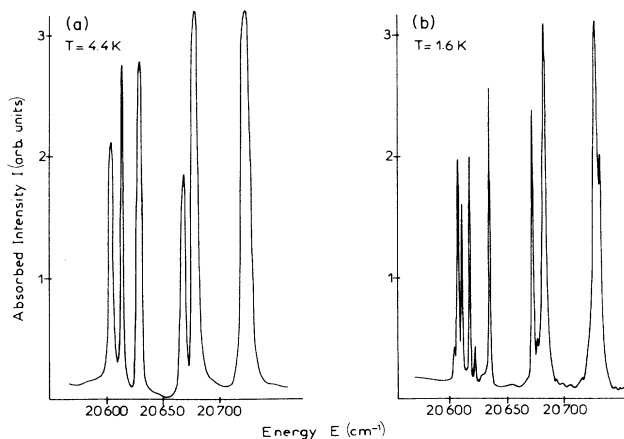


FIG. 1. Absorption spectra of TbF_3 for the ${}^7F_6 \rightarrow {}^5D_4$ transitions of Tb^{3+} at 4.4 and 1.6 K. In the ferromagnetically ordered phase at 1.6 K, the three “quasidoublets” of the 5D_4 multiplet have been spontaneously split showing the presence of Tb^{3+} - Tb^{3+} interactions.

TABLE I. Positions (λ and ν) and linewidths ($\Delta\nu$) of the absorption lines for the transitions ${}^7F_6 \rightarrow {}^5D_4$ in the ferromagnetically ordered (1.6 K) and disordered (4.4 K) phases of TbF_3 .

1.6 K			4.4 K			
λ (Å)	ν (cm^{-1})	$\Delta\nu$ (cm^{-1})	Symmetry	λ (Å)	ν (cm^{-1})	$\Delta\nu$ (cm^{-1})
4822.15	20731.8		A'			
4823.1	20727.8		A''	4823.35	20726.7	11
4833.5	20683.2	3.7	A''	4833.8	20681.9	7
4836.0	20672.5	1.3	A'	4836.35	20671	6
4844.9	20634.5	1.3	A''	4845.15	20633.4	6
4847.85	20621.9	0.8	A'			
4849.0	20617.05	0.8	A''	4848.85	20617.7	3
4850.4	20611.1	0.8	A'			
4851.2	20607.7	1.3	A'	4851.25	20607.5	5

significant ultraviolet emission¹⁵ attributed to the ${}^5D_3 \rightarrow {}^7F_J$ transitions of Tb^{3+} and for a nonexponential decay of the incoherent exciton which was observed under high excitation density. The anti-Stokes fluorescence intensity was observed to rise rapidly (70 nsec) and to decay exponentially with a time constant of 89 μsec , half the 5D_4 exciton lifetime, in excellent agreement with the rate-equation model.¹⁵ Finally, the exciton-exciton annihilation rate provides another determination of the effective diffusion coefficient¹⁵ in agreement with the previous one.¹¹

B. Fluorescence properties below T_C

1. Observed spectra

The absorption spectrum recorded at 1.6 K is presented in Fig. 1(b). Due to the greater sharpness of the lines relative to those observed at 4.4 K, the nine Stark components of the 5D_4 manifold in C_s symmetry were well resolved. Their positions and linewidths are summarized

in Table I. By comparison with the absorption spectrum recorded at 4.4 K we note the presence of three singlets (20633.4, 20671, and 20681.9 cm^{-1}) and three "quasi-doublets" (20607.5, 20617.7, and 20726.7 cm^{-1}). The 1.6-K absorption spectra recorded with linearly polarized laser light and an oriented sample allowed determination of the symmetry A' or A'' of each 5D_4 Stark component, assuming the nature of the ground state to be $M_J = \pm 6$.

It is also interesting to note that the three singlets shift about 1.3 cm^{-1} to higher energy relative to their positions in the 4.4-K absorption spectrum, and that there is an asymmetry on the low-energy side of each main line. This sharpening, with a shift to higher energy and a clear asymmetry, was observed when the sample reached the ordering temperature and can be attributed to the effect of interactions between Tb^{3+} ions in the ground state. As recently discussed by H \ddot{u} fn \ddot{u} r¹⁶ for the case of TbF_3 , these magnetic interactions may be reasonably described by a so-called molecular field which is produced by the neighboring Tb^{3+} ions. This molecular field has consequences similar to those of an external real magnetic field, leading to a splitting of degenerate crystal-field energy levels in the ordered phase of the material. In TbF_3 , the lowest crystal-field level of the 7F_6 ground multiplet is an accidental doublet which is split in the ordered state, and which may then be described as a $M_J = \pm 6$ or spin- $\frac{1}{2}$ Ising system as described in Sec. II above.

Assuming that the short-range interactions are along chains, each ion interacts predominantly with only two neighbors above T_C where there is only short-range order. Thus each sublevel appearing in the absorption spectrum to a true 5D_4 singlet state indicates a possible magnetic configuration of the two Tb^{3+} nearest neighbors. Following H \ddot{u} fn \ddot{u} r,¹⁶ this splitting is a few wave numbers at 4.4 K, and the population of each sublevel, given by the Boltzmann distribution, causes an apparent broadening of the excitation or absorption lines. (The spin fluctuations of more distant ions can also contribute to the true line broadening.)

Below T_C , the magnetic dipole-dipole interaction, which is long ranged, makes a substantial contribution to the molecular field. At 1.6 K, the molecular field has increased significantly, and this leads to an increase in the total ground-state splitting. Due to the very low tempera-

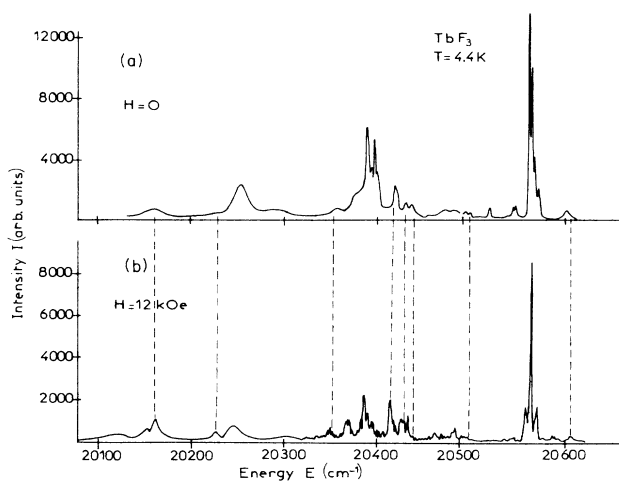


FIG. 2. Emission spectra for the ${}^5D_4 \rightarrow {}^7F_6$ transition of Tb^{3+} ions in TbF_3 at 4.4 K. Dotted lines indicate the position of the intrinsic emission lines. Other fluorescence lines arise from trap emission.

ture, only the lowest sublevel is populated. This results in the observed sharpening and in a further shift to higher energy of the excitation lines.

The blue emission spectrum at 1.6 K for the ${}^5D_4 \rightarrow {}^7F_6$ transition shown in Fig. 3(a) was recorded with selective excitation in one of the nine 5D_4 Stark components. As at 4.4 K, we note the presence of several groups of lines, but now they are better resolved. Indeed, the deep-trap ($\Delta_0 \approx 40 \text{ cm}^{-1}$) fluorescence is composed of two main lines located at $20\,561.5 \text{ cm}^{-1}$ and $20\,553.9 \text{ cm}^{-1}$ showing a ground-state splitting of 7.6 cm^{-1} . Moreover, the intensity of these trap lines (due to perturbed Tb^{3+} ions) has decreased on behalf of the intrinsic ones and a new group of lines, arising from the emission of shallow traps ($\Delta_1 \approx 10 \text{ cm}^{-1}$), appears at $20\,592.4 \text{ cm}^{-1}$ and $20\,584.8 \text{ cm}^{-1}$. This shallow-trap fluorescence also shows a ground state splitting of 7.6 cm^{-1} . At this point, it is interesting to remark that this splitting is identical to the one observed recently by Brinkmann and Hühner on an optical absorption transition from the magnetic Tb^{3+} ground state to a singlet excited state of the 5D_4 multiplet in TbF_3 at 1.6 K.¹⁶

We also note the presence of three lines located at

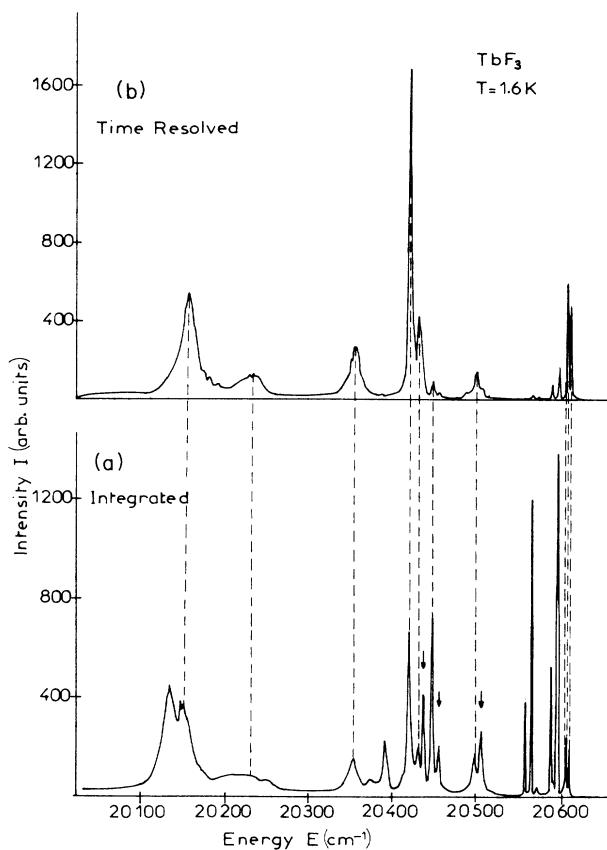


FIG. 3. Emission spectra for the ${}^5D_4 \rightarrow {}^7F_6$ transitions of Tb^{3+} ions in TbF_3 at 1.6 K. Dotted lines indicate the position of the intrinsic emission lines. The small arrows show the lines arising from the fluorescence of negative binding energy "traps."

$20\,502.9$, $20\,448.8$, and $20\,431.2 \text{ cm}^{-1}$ which are indicated by arrows in Fig. 3 and which were not observed at temperatures greater than T_C . These lines correspond to "trap" levels located above the intrinsic levels by $\Delta \approx -11 \text{ cm}^{-1}$.

Finally, we conclude this discussion of the energy levels by noting that each emission line of the spectrum presented in Fig. 3(a) provides the same excitation spectrum which duplicates exactly the absorption spectrum of the crystal. This is expected since intrinsic ions are far more numerous than perturbed ones.

2. Fluorescence dynamics

The dynamical properties of this 1.6-K visible fluorescence are significantly different from those observed at 4.4 K as one may readily see from a comparison of Figs. 4(a) and 4(b). Indeed the decay of the intrinsic emission line located at $20\,607.7 \text{ cm}^{-1}$ presented in Fig. 4(a) is exponential with a time constant of 1.6 msec, a value one order of magnitude longer than at 4.4 K. In agreement with this time dependence, the intensity of the trap line situated at $20\,561.5 \text{ cm}^{-1}$ exhibits an initial rise for 2.5 msec as shown in Fig. 4(d) and then decreases exponentially with a time constant of 6 msec as shown in Fig. 5. The latter value characterizes the radiative lifetime of Tb^{3+} visible fluorescence in TbF_3 . Accordingly, by using time-resolved spectroscopy, it is easy to eliminate the fluorescence lines due to perturbed Tb^{3+} ions in the emission spectrum. With a delay of 500 nsec and an electronic gate of $200 \mu\text{sec}$, the intrinsic emission lines dominate the observed spectrum as shown in Fig. 3(b). The measured 7F_6 crystal-field splittings were identical to the ones obtained previously at 4.4 K.¹¹

As for higher temperatures, an ultraviolet anti-Stokes fluorescence was observed by exciting the 5D_4 states, and it is again attributed to the ${}^5D_3 \rightarrow {}^7F_6$ transitions since the relative positions of the main lines exactly match the 7F_6 ground multiplet splitting at 1.6 K. The visible excitation spectrum of the anti-Stokes emission again duplicates the

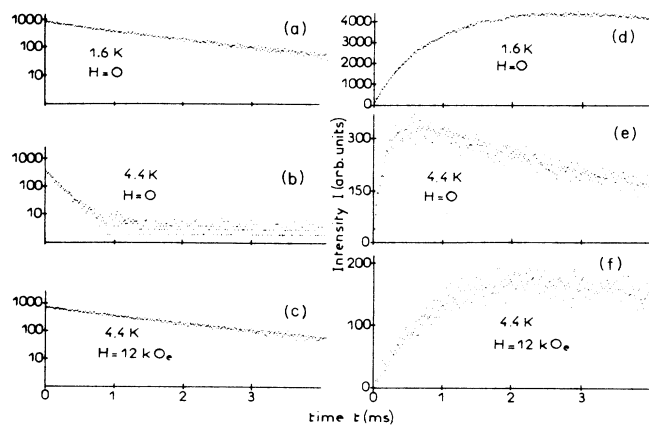


FIG. 4. Decay for an intrinsic line (a), (b), and (c) and a trap line (d), (e), and (f) in TbF_3 . [Note that (a), (b), and (c) have log scales, while (d), (e), and (f) do not.]

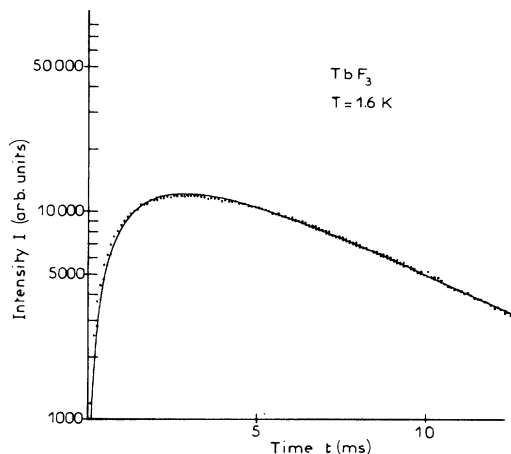


FIG. 5. Decay of the trap line ($20\,561.5\text{ cm}^{-1}$) at 1.6 K in TbF_3 : \cdots , experimental data; — , fitting using Eq. (6).

absorption spectrum as well as the excitation spectra of the intrinsic and trap Stokes fluorescences. The anti-Stokes fluorescence intensity exhibits a fast risetime, and then decays exponentially with a time constant of $740\ \mu\text{sec}$, again just half the value of the 5D_4 incoherent exciton lifetime at the same temperature.

All these results suggest that the same processes are taking place at both 4.4 and 1.6 K. Thus, we should be able to use the rate equation model to describe the overall dynamics of the fluorescence in the magnetically ordered phases of TbF_3 .

C. Spectroscopy at 4.4 K with an applied magnetic field

From magnetic measurements,¹² it is known that, below $T_C = 3.95\text{ K}$, the Tb^{3+} magnetic moments in TbF_3 spontaneously align with a net ferromagnetic component along the *a* direction. At 4.4 K, an external magnetic field *H* applied parallel to *a* also tends to align the spins along this axis. So, for a given value of *H* we may hope to observe nearly the same fluorescence spectra as when the sample is cooled down to 1.6 K. The time resolved fluorescence measurements under these conditions add considerable insight into the excited state dynamics. We also present the experimental results obtained with the external magnetic field applied along the *c* direction.

1. *H* parallel to *a*

We have seen that at 4.4 K and zero field the most intense emission lines were those coming from perturbed Tb^{3+} ions as shown in Fig. 2(a). When the applied magnetic field is increased, the intensity of these trap lines drops on behalf of the intrinsic lines. This can be seen by comparing the spectrum recorded with $H = 12.2\text{ kOe}$ [Fig. 2(b)] with the zero-field one [Fig. 2(a)]. In each case the dotted lines indicate the intrinsic emission lines. A new group of lines appears around $20\,593\text{ cm}^{-1}$ arising from the shallow traps with energy levels located at about 10 cm^{-1} below the intrinsic ones.

The excitation spectrum of the deeper trap emission ($\Delta_0 \approx 40\text{ cm}^{-1}$) was recorded for various values of *H*. For a 4-kOe magnetic field, the three quasidoublets observed at zero field were resolved and the total 5D_4 splitting was nominally the same as that obtained at 1.6 K without any applied magnetic field. When *H* increases, the splitting of these three quasidoublets becomes larger.

The decay of the intrinsic fluorescence intensity was recorded with different values of the applied magnetic field *H*. With increasing *H*, the decay becomes progressively longer, and for $H = 12.2\text{ kOe}$ it is exponential with a time constant of 1.66 msec [see Fig. 4(c)]. Correspondingly, the time evolution of the deep trap emission intensity changes when the applied magnetic field is increased. The time t_M at which this fluorescence reaches its maximum becomes larger, evolving from 0.5 msec for $H = 0$ [Fig. 4(e)] to 2.5 msec for $H = 12.2\text{ kOe}$ [Fig. 4(f)].

At this point, it is important to note that both the decays and the emission spectra at 4.4 K, with an applied magnetic field of 12.2 kOe along the easy axis of magnetization *a*, are similar to those observed when the sample is cooled down to 1.6 K. [Compare Figs. 4(a) and 4(c) with Figs. 4(d) and 4(f)].

2. *H* parallel to *c*

The application of a magnetic field along the *c* crystallographic direction at 4.4 K does not have the same effect on the dynamical properties of Tb^{3+} fluorescence in TbF_3 . Indeed, the incoherent exciton lifetime remains the same ($180\ \mu\text{sec}$) even with an applied magnetic field of 25 kOe. That is, there is no change of the fluorescence dynamics at 4.4 K with an applied magnetic field along the *c* direction up to 25 kOe.

This behavior may be understood by looking at the magnetization as a function of applied magnetic field parallel to *c*. The experimental data of Ref. 12 suggest a smooth variation of the magnetic susceptibility as the temperature increases in the range of 4.4 K. As a consequence, it would be necessary to apply a much stronger magnetic field along the *c* direction in order to induce significant effects at 4.4 K.

IV. DISCUSSION

The experimental results concerning the fluorescence properties of TbF_3 in its ferromagnetic phase show that the intrinsic emission has increased with a consequent reduction of the trap fluorescence. Throughout the temperature range from 300 to 1.6 K the decay mode is always exponential. Thus, to describe the overall exciton-to-trap energy-transfer process in this material at 1.6 K, we may use the well-known fast-diffusion model in which the excitation transfers between the various levels are expressed in terms of transition rates. A general presentation of this model has been given in a previous paper to explain the dynamical properties of the fluorescence of TbF_3 at 4.4 K.¹¹ The principal levels of interest at 4.4 K are the exciton band (level 2), the shallow-trap level (level 1) located at $\Delta_1 \approx 10\text{ cm}^{-1}$ below the exciton band, and the deep-trap level (level 0) separated from the exciton band by $\Delta_0 \approx 40\text{ cm}^{-1}$. At 1.6 K, we must take into ac-

count the perturbed Tb^{3+} levels (level 3) located at energies higher than the exciton band. Indeed, we have mentioned in Sec. III B the presence of three new emission lines at this temperature, each located at about 11 cm^{-1} on the high-energy side of an intrinsic emission line. Thus, in the ferromagnetic phase of TbF_3 the rate equations [Eq. (6) of Ref. 11] become

$$\frac{dN_2}{dt} = (W_r + W_{21} + W_{20} + W_q + W_{23})N_2 + N_f AI, \quad (1)$$

$$\frac{dN_1}{dt} = W_{21}N_2 - W_r N_1, \quad (2)$$

$$\frac{dN_0}{dt} = W_{20}N_2 - W_r N_0, \quad (3)$$

$$\frac{dN_3}{dt} = W_{23}N_2 - W_3 N_3. \quad (4)$$

W_{23} is the transition rate from level 2 to level 3, and the population N_3 decreases at the rate W_3 . We have neglected the backtransfer rate W_{12} due to the small value of $e^{-\Delta_1/kT}$ at 1.6 K. After the excitation pulse, we obtain the following expressions for the time evolution of population N_2 and N_0 :

$$N_2(t) = N_2(0)e^{-(W_r + W_{21} + W_{20} + W_q + W_{23})t}, \quad (5)$$

$$N_0(t) = \frac{W_{20}N_2(0)}{W_{23} + W_{21} + W_{20} + W_q} \times (e^{-W_r t} - e^{-(W_r + W_{21} + W_{20} + W_q + W_{23})t}). \quad (6)$$

We have experimentally measured the incoherent-exciton lifetime to be $\tau = 1.6$ msec which corresponds to $(W_r + W_{21} + W_{20} + W_q + W_{23})^{-1}$ following Eq. (5). As a test of the validity of this model, that value was used to describe the decay profile of the deep trap with the aid of Eq. (6). The comparison to the data is shown in Fig. 5. It gives quite satisfactory agreement with the experiment using the known value $W_r = 167 \text{ sec}^{-1}$. The fast diffusion regime thus appears to be appropriate below the ferromagnetic phase transition, as well as above.

The key question arising in this work is thus: *Why does the incoherent-exciton lifetime τ increase by one order of magnitude between 4.4 K and 1.6 K?*

In the fast diffusion regime, the time constant τ characterizing the incoherent-exciton decay is connected with an effective diffusion coefficient D in the following way:

$$\tau^{-1} = \tau_0^{-1} + 4\pi DN_a \rho, \quad (7)$$

where τ_0^{-1} is the radiative rate, N_a is the trap concentration, and ρ is a length which characterizes the relative effectiveness of direct transfer and migration to traps. This relation [Eq. (7)] suggests that the change of τ below the Curie temperature corresponds to a decrease of the coefficient D . This could arise either by a decrease of the resonant energy transfer between intrinsic ions or by a reduction of the energy transfer probability of the last step between intrinsic and trap ions.

A. Reduction of resonant energy transfer

At both 4.4 and 1.6 K the observed absorption linewidth can be understood using a simple model involving the interactions between nearest neighbors.¹⁶ Following Hufner, at 4.4 K the Tb^{3+} ground state is composed of three levels, because configurations of neighboring ions have various arrangements from pure ferromagnetic to pure antiferromagnetic.¹⁶ The population of the different levels is given by the Boltzmann distribution, but the splitting cannot be observed because of the homogeneous broadening of the lines (6 cm^{-1}) due to spin fluctuations. As the temperature decreases below T_C , the molecular field further removes the degeneracy of the possible spin configurations, leading to the observation of four absorption lines. Moreover, since the spins tend to be aligned, there is an effective narrowing of the homogeneous linewidth. At 4.4 K and above with an external magnetic field, all the spin-configuration degeneracy is again completely removed, and a 4-kOe applied magnetic field induces an overall splitting of the same order of magnitude as that occurring spontaneously at 1.6 K. However, because of the higher temperature (4.4 K) the homogeneous broadening of the lines should be different, and it is necessary to apply a higher magnetic field in order to achieve the experimental conditions observed at 1.6 K.

Based on these considerations, we may propose to attribute the decrease of the energy migration to a reduction of the quaresonance between excited levels of intrinsic ions when either the temperature drops to 1.6 K or a 12.2 kOe external magnetic field is applied at 4.4 K. That is, in well-ordered states the homogeneous linewidth becomes small enough compared to the inhomogeneous broadening due to strain that resonant energy transfer is "frozen out." If this picture involving a "quasilocalization" of the excitation is true, it provides some evidence for a "microscopic" inhomogeneous broadening.

B. Reduction of transfer to traps

Another possible consequence of the magnetic ordering and the magnetically induced splittings involves the probability for trapping. The fluorescence spectrum recorded at 1.6 K [Fig. 3(a)] shows clearly the existence of perturbed Tb^{3+} levels located at an energy higher than the corresponding intrinsic Tb^{3+} level. These perturbed Tb^{3+} ions did not exhibit any fluorescence at 4.4 K.

Consider the excitation energy transfer between an intrinsic ion i and a negative-binding-energy "trap" t whose energy levels are located 11 cm^{-1} higher than the corresponding intrinsic levels. A thermally induced population of the upper-ground-state component of the perturbed ions is necessary to achieve efficient energy transfer. Otherwise, the energy mismatch is larger than the linewidth. At the upper range of liquid-helium temperatures where the TbF_3 is not magnetically ordered, this requirement is well satisfied, leading to efficient energy transfer between intrinsic ions i and the negative-binding-energy "traps" as shown in Fig. 6(a). As these "trap" ions can participate in the energy diffusion process but are small in number

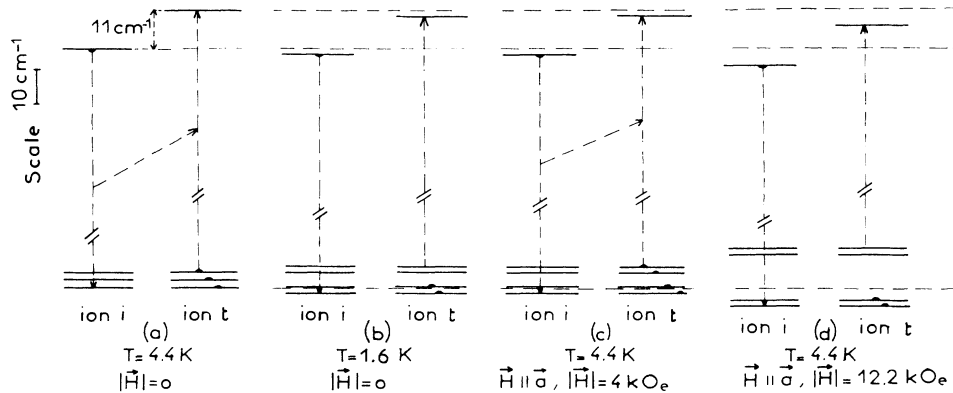


FIG. 6. Energy levels of the intrinsic i and negative binding energy "trap" t Tb^{3+} ions in TbF_3 involved in the barrier model.

compared to the intrinsic ions, they do not generate any observable fluorescence at 4.4 K.

On the other hand, at 1.6 K, the material is in its ferromagnetic phase, and the upper level of the Tb^{3+} ground state has very little population. "Trap" ions t could thus play the role of a barrier for the diffusion process as shown in Fig. 6(b). The barrier role is plausible for the following reasons. Various deep and shallow traps will be formed in the neighborhood of an impurity or vacancy. The deep traps will presumably be Tb^{3+} ions which are first neighbors to the impurity and which are thus strongly perturbed. These deep traps will be surrounded by more weakly perturbed ions which become shallow traps ($\Delta \approx \pm 11 \text{ cm}^{-1}$). Finally beyond that more distant shell, the Tb^{3+} ions are very weakly perturbed and thus are intrinsic. From this perspective, the negative-binding-energy "traps" t would lie between the intrinsic ions and the deep traps and assume the barrier role. That would reduce the efficiency of the trapping at this temperature giving rise to an incoherent-exciton lifetime longer than at 4.4 K.

Figures 6(c) and 6(d) show the ground and first excited levels of intrinsic i and "trap" t Tb^{3+} ions with an applied magnetic field parallel to the a axis at 4.4 K. When $H = 4 \text{ kOe}$, the ground state splitting is identical to the one measured at 1.6 K, but, due to the Boltzmann distribution, the higher level of the ground state is also populated and the excitation energy would be easily transferred from intrinsic ions i and "trap" ions t . However, since the splitting is increasing with the field, at 12.2 kOe it would no longer be possible to go through the barrier efficiently for the feeding of the other traps. The barrier role of the "trap" t can possibly explain the fluorescence dynamics of TbF_3 in all the experiments described above.

V. SUMMARY

The dynamical properties of the fluorescence of TbF_3 have been investigated above and below the ferromagnetic ordering temperature. The significant (factor of ten) lengthening of the incoherent-exciton decay gives strong evidence for a decrease of the diffusion between intrinsic ions and (or) a decrease of the trapping probability for perturbed Tb^{3+} ions. The role of the nearest neighbor interactions is pointed out, taking advantage of the previous studies of the ground state magnetic splitting involving a pseudo doublet (mainly $M_J = \pm 6$). In the related compound $TbAlO_3$, which is known to order antiferromagnetically below 3.8 K, we have already reported⁷ the experimental evidence for a strong localization of the optical excitation at 1.6 K. In a forthcoming paper, we shall compare the behavior of Tb^{3+} fluorescence properties in several concentrated compounds where the temperature reaches the magnetic transition point, and we shall discuss the nature of the coupling between neighboring intrinsic ions in ground and excited states giving rise to the diffusion of the optical excitation.

ACKNOWLEDGMENTS

We are grateful to M. Robinson (Hughes Laboratory, U.S.A.) for having kindly provided us with the single crystals used here and also to J. C. Viala and Y. Lecoq for having oriented the samples. Thanks are also expressed to the Laboratoire de Spectrometrie Physique de Grenoble (France) for having lent the superconducting magnet to us. We also acknowledge helpful conversations with F. Auzel, R. M. Macfarlane, and R. S. Meltzer. The Laboratoire de Physico-Chimie des Matériaux Luminescents is "Unité associée no. 442 au Centre National de la Recherche Scientifique."

¹R. S. Meltzer and H. W. Moos, Phys. Rev. B **6**, 264 (1972).

²R. L. Cone and R. S. Meltzer, Phys. Rev. Lett. **30**, 859 (1973); Phys. Rev. B **13**, 2818 (1976).

³J. K. Kjems, G. Shirane, R. J. Birgeneau, and L. G. Van Uitert, Phys. Rev. Lett. **21**, 300 (1973); R. J. Birgeneau, R. K. Kjems,

G. Shirane, and L. G. Van Uitert, Phys. Rev. B **10**, 2512 (1974); K. B. Lyons, R. J. Birgeneau, E. I. Blount, and L. G. Van Uitert, *ibid.* **11**, 891 (1975).

⁴R. L. Cone and R. S. Meltzer, J. Chem. Phys. **62**, 3575 (1975); R. S. Meltzer and R. L. Cone, J. Lumin. **12/13**, 247 (1976);

- R. S. Meltzer, *Solid State Commun.* **20**, 553 (1976); H. T. Chen and R. S. Meltzer, *Phys. Rev. Lett.* **44**, 599 (1980).
- ⁵H. B. Ergun, K. A. Gehring, and G. A. Gehring, *J. Phys. C* **9**, 1101 (1976).
- ⁶M. F. Joubert, C. Linares and B. Jacquier, Proceedings of the IIIrd European Conference on Solid State Chemistry, Regensburg, 1986 (unpublished).
- ⁷M. F. Joubert, C. Linares, B. Jacquier, and B. Wanklyn, *J. Lumin.* **31/32**, 90 (1984).
- ⁸J. P. Van Der Ziel, and L. G. Van Uitert, *Solid State Commun.* **7**, 819 (1969).
- ⁹J. P. Van Der Ziel, L. Kopf, and L. G. Van Uitert, *Phys. Rev. B* **6**, 815 (1972).
- ¹⁰A. Zalkin and D. H. Templeton, *J. Am. Chem. Soc.* **75**, 2453 (1953).
- ¹¹M. F. Joubert, B. Jacquier, R. Moncorge, and G. Boulon, *J. Phys. (Paris)* **43**, 893 (1982).
- ¹²L. Holmes, H. J. Guggenheim, and G. W. Hull, *Solid State Commun.* **8**, 2005 (1970).
- ¹³M. Piotrowski and A. Murasik, *Phys. Status Solidi A* **60**, K195 (1980).
- ¹⁴L. A. Bumagina, B. N. Kazakov, B. Z. Malkin, and A. L. Stolv, *Fiz. Tverd. Tela (Leningrad)* **19**, 1073 (1977) [*Sov. Phys.—Solid State*, **19**, 624 (1977)].
- ¹⁵M. F. Joubert, B. Jacquier, and R. Moncorge, *Phys. Rev. B* **28**, 3725 (1983).
- ¹⁶S. Hufner, in *Systematics of the Properties of the Lanthanides*, edited by S. P. Sinha (Reidel, Dordrecht, 1982), pp. 313–388.